

# Significance of MPEG-7 Textural Features for Improved Mass Detection in Mammography

Nevine H. Eltonsy, Georgia D. Tourassi *Member, IEEE*, Aleksey Fadeev, Adel S. Elmaghhraby *Senior Member, IEEE*

**Abstract**—The purpose of the study is to investigate the significance of MPEG-7 textural features for improving the detection of masses in screening mammograms. The detection scheme was originally based on morphological directional neighborhood features extracted from mammographic regions of interest (ROIs). Receiver Operating Characteristics (ROC) was performed to evaluate the performance of each set of features independently and merged into a back-propagation artificial neural network (BPANN) using the leave-one-out sampling scheme (LOOSS). The study was based on a database of 668 mammographic ROIs (340 depicting cancer regions and 328 depicting normal parenchyma). Overall, the ROC area index of the BPANN using the directional morphological features was  $Az = 0.85 \pm 0.01$ . The MPEG-7 edge histogram descriptor-based BPNN showed an ROC area index of  $Az = 0.71 \pm 0.01$  while homogeneous textural descriptors using 30 and 120 channels helped the BPNN achieve similar ROC area indexes of  $Az = 0.882 \pm 0.02$  and  $Az = 0.877 \pm 0.01$  respectively. After merging the MPEG-7 homogeneous textural features with the directional neighborhood features the performance of the BPANN increased providing an ROC area index of  $Az = 0.91 \pm 0.01$ . MPEG-7 homogeneous textural descriptor significantly improved the morphology-based detection scheme.

**Keywords** Computer Assisted Detection (CAD), MPEG-7 textural descriptors, malignant masses, morphological features.

## I. INTRODUCTION

THE present study investigates the performance of MPEG-7 textural descriptors for the automated detection of mammographic masses. Textural descriptors are powerful low-level features and are frequently used for content-based image retrieval systems [1]. Textural descriptors are often used to describe contrast, coarseness, and local edges and directionality to account texture. Efforts to combine textural features in the area of image retrieval for medical applications are also made. The focus of this study is to evaluate the MPEG-7 textural descriptors before merging them with our automated morphology-based features reported before for improving detection of masses in screening mammograms. A detailed overview of the textural descriptors of MPEG7 is provided in [2]. MPEG-7 descriptors were widely used for image processing and searching before they were recently incorporated into video analysis, classification and image retrieval [3]-[5]. In this work we are basically evaluating two of the MPEG-7 textural descriptors namely: edge histogram descriptor

(EHD) [6], and homogeneous texture descriptor (HTD) [7,8].

In a previous study for the detection of masses in screening mammography, we presented the directional neighborhood features extracted from eight main directions from the center suspicious mammographic locations [9]. That study capitalized on tracking the morphological directional characteristics of a group of pixels that are strongly connected to the pixel values at the center of a region of interest (ROI) in basically eight directions. The study was performed using a database of 1,337 mammographic ROIs extracted from the digital database for screening mammograms (DDSM). The extracted directional neighborhood features were merged into a BPANN. We analyzed the performance of the network using Receiver Operator Characteristics (ROC) analysis. In this work, we investigate MPEG-7 texture descriptors before and after merging them with our morphological features.

The sections in this paper are organized as follows: Section 2 introduces the dataset used in this study. Section 3 describes the directional features and the MPEG-7 descriptors used in this study. Results are presented in section 4. Conclusion and discussion of future work are presented in section 5.

## II. DATASET

The dataset used in this study was collected from the digital database for screening mammography (DDSM) [10]. Only images digitized using Lumisys scanner were downloaded and archived. Mammograms containing malignant masses with biopsy-proven pathological ground truth were used. The DDSM cases included the physicians' annotations around detected masses. 512x512 pixel regions of interests (ROIs) centered the physician' annotations were extracted for a total of 340 mass ROIs. In addition, 328 ROIs were extracted depicting normal breast parenchyma from the normal DDSM mammograms included in volumes "normal\_09", and "normal\_10". In total, 668 ROIs were used to examine the significance of the MPEG-7 edge histogram descriptor (EHD) and homogeneous histogram descriptor (HTD) over the previous morphological directional neighborhood (DN) features for the computer-assisted detection of malignant masses in screening mammograms.

### III. METHODS

#### A. Directional Neighborhood Features

The directional neighborhood analysis (DNA) CAD scheme is designed to track the propagation of pixel values related to the center pixel value of the ROI, assuming that the 512x512 is originally centered on the annotated mass lesion. The scheme assumes that pixel values within 2% error from the center pixel value of the ROI are strongly connected. Since malignant masses tend to disturb the normal breast parenchymal structure, the morphological characteristics of those strongly connected pixels should capture the disturbances. The morphological characteristics are studied from eight directions starting from the center of the ROI and propagating radially and bilaterally covering the ROI from every direction. A total of eight morphological features are collected per direction. The feature vector per ROI is then represented as the average of each feature across the eight directions. DNA is described in detail in [9]. Figure 1 illustrates the directional neighborhood propagation scheme. The figure shows a normal ROI along with the directional neighborhood propagation in (Fig. 1a,b) respectively. Figure (1c,d) shows a malignant mass with its corresponding propagation characteristics.

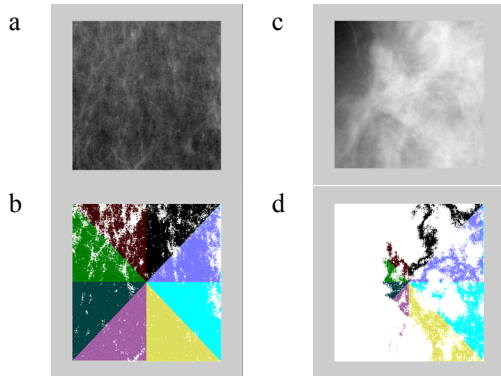


Fig. 1: (a) Normal ROI (b) visual representation of the DN propagation in Fig. 1a (c) Malignant ROI (d) visual representation of the directional neighborhood propagation in Fig. 1c

#### B. MPEG-7 Edge Histogram Descriptor (EHD)

The Edge Histogram Descriptor employed in this study is based on the work of Won et al. [6]. The EHD basically represents the frequent distribution “histogram” of 5 types of edges for 30 sub-images. Basically, the first 16 sub-images represent the local EHD with total of 80 bins (16x5 bins), 1 global EHD (1x5 bins), and the final 13 sub-images are used to calculate the semi-global EHD with total of 65 bins (13x5 bins). Five bins then represent each sub-image as they represent the histogram of the 4 directional edges and one non-edge with a total of 150 bins. Within each sub-image the edge types represent vertical, horizontal, diagonal, anti-diagonal, and non-directional edge. Each sub-image is filtered by each directional and non-directional mask (see

Figure 2). Edge histogram information is extracted using the average edge value in each 2x2 block as a basic element. Thus, the histogram for each sub-image represents the relative frequency of occurrence of the 4 edge and non-edge types in the corresponding sub-image. Figure 3 presents the 5 edge detector operators applied as mask on each 2x2 block element in every sub-image.

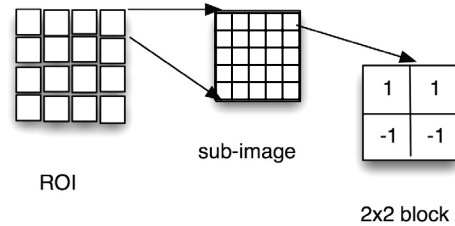


Fig. 2. Partitioning of an ROI into 16 sub-images and image blocks showing example of sub-block with horizontal detector operator for the local EHD.

$1 \begin{vmatrix} 1 & -1 \\ 1 & -1 \end{vmatrix}$	$1 \begin{vmatrix} 1 & 1 \\ -1 & -1 \end{vmatrix}$	$\sqrt{2} \begin{vmatrix} 0 & 0 \\ 0 & -\sqrt{2} \end{vmatrix}$	$0 \begin{vmatrix} \sqrt{2} & 0 \\ -\sqrt{2} & 0 \end{vmatrix}$	$2 \begin{vmatrix} 2 & -2 \\ -2 & 2 \end{vmatrix}$
--	--	---	---	--

Fig. 3. Type of edge detector operators in order from left to right vertical, horizontal, diagonal, anti-diagonal, and non-edge operator

Figure 4 represents the partitioning of the 13 sub-images for the semi-global histograms while the global edge histogram represents the 5 edge histogram bins computed from all over the ROI. At the end, each bin represents the number of blocks found when corresponding edge or non-edge is dominant. As a result, a total of 150 histogram bins summarize the edge histogram descriptor for each ROI.

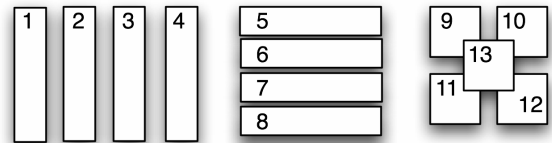


Fig. 4. Partitioning of the 13 sub-images used for the calculation of semi-global histograms

#### C. Homogeneous Textural Descriptor (HTD)

Gabor filters are well known for texture analysis and have been used in several studies. In this work we used the calculation of HTD reported in [7] and [8]. For textural analysis, frequency elements, as obtained by Fourier transformations, are an important part of an image. The homogeneous texture descriptor consists of the mean, standard deviation of the ROI along with the energy and energy deviation features obtained from 30 channels as in [7]. The texture descriptors are the first and the second moments of energy in each channel. The frequency layout is obtained by taking the Radon transform on an ROI and subsequent 1D Fourier transform on the data. In [8], the

bank of Gabor filters was generated by partitioning frequency space into 12 angular directions and using 9 filters in radial direction, instead of 6 angular directions and 5 radial filters used in [7]. Figure 5 shows the MPEG-7 Gabor Filters using the 30 and 120 channels in parts a and b respectively. Mathematically, let radial index be  $s = 0 \dots 8$  and angular index be  $r = 0 \dots 11$ , then filters are defined as:

$$G_{P_{s,r}}(\omega, \theta) = \exp\left[\frac{-(\omega - \omega_s)^2}{2\sigma_{\omega_s}^2}\right] \cdot \exp\left[\frac{-(\theta - \theta_r)^2}{2\sigma_{\theta_r}^2}\right]$$

where,

$$\theta_r = \frac{\pi}{12}r, \quad \sigma_{\theta_r} = \frac{\pi}{12 \cdot 2 \cdot \sqrt{2 \ln 2}},$$

$$\omega_s = \frac{1}{32} + \frac{s^2}{80}, \quad \sigma_{\omega_s} = \frac{1/32 + s^2 / 80}{(3 + s^2 / 25)\sqrt{2 \ln 2}}$$

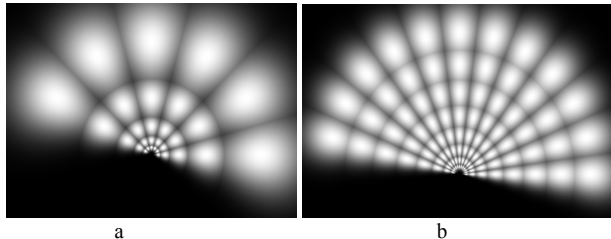


Fig. 5. (a) MPEG-7 Gabor filters based on 30 (6x5) channels with total of 62 features [7] (b) MPEG-7 Gabor filters based on 120 (12x9) channels with total of 218 features [8]

#### D. Classification

For each of the above feature sets, we merged the features extracted into a decision to discriminate the normal regions from malignant regions using a back-propagation artificial neural network (BPANN). The network worked as a non-linear classifier [11] trained using Levenberg-Marquardt algorithm [12] suitable for pattern recognition tasks. Leave-one-out sampling scheme was used to train and test the network [13]. The performance of the BPANN was evaluated using Receiver Operating Characteristics (ROC) analysis. ROC area statistical tests were used to show if features extracted from one method are statistically more discriminatory than features extracted from the other method. We used the ROCKIT software (Charles Metz, Univ. of Chicago) to fit ROC curves to the BPANN outputs and perform statistical analysis.

#### IV. RESULT

The results are summarized in Table 1 where we present the ROC area index for each network. Overall, DNA features and the homogeneous texture descriptor using either 30 channels, and 120 channels have Az areas that are significantly higher than the area index achieved using the edge histogram descriptor features. DNA features and HTD features have similar Az areas, with HTD being slightly better than DNA but not significant. However, there is low correlation between the ROC performance of the neural

networks, suggesting that DNA and HTD capture different type of image information. This finding is expected due to the inherent differences of both feature sets (morphological vs. textural). There is no significant difference between HTD using 30 channels and HTD with 120 channels as the difference in area index was small and correlation between both techniques was high. Therefore, we expect that they capture similar image content.

The above results suggest that combining DNA features with HTD should improve the Az area index because of their low correlation ( $r = 0.06$ ). Consequently, we merged the eight DNA features with the HTD (30 channels resolved in 62 features) into a single BPANN using the same algorithm and the leave-one-out sampling scheme as before. The total number of merged features was 70 (8 DNA + 62 HTD). The ROC performance of the BPANN network using all the 70 features was  $Az = 0.91 \pm 0.01$ . This performance was statistically significantly better than the ones achieved using either the DNA or the HDT features alone. Figure 6 shows the ROC curves of the four networks using the DNA, HTD with 30 channels, HTD with 120 channels, as well as the merged features.

**Table 1.** Results of ROC Analysis

Method Extractor (328-Normal vs 340-Cancer) ROIs	Feature vector per ROI	BPANN – ROC Area Index Az =
Directional Neighborhood Analysis (DNA)	1 x 8	$Az = 0.85 \pm 0.01$
Edge Histogram Descriptor (EHD)	1 x 5	$Az = 0.71 \pm 0.01$
Homogeneous Texture Descriptor (HTD)	1 x 62	$Az = 0.88 \pm 0.02$
Homogeneous Texture Descriptor (HTD)	1 x 218	$Az = 0.88 \pm 0.01$
Merged DNA & HTD	1 x 70	$Az = 0.91 \pm 0.01$

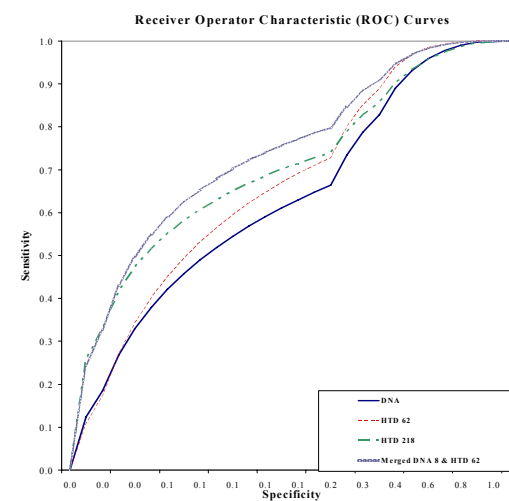


Fig. 6. ROC area index of DNA, HTD with 30 channels, HTD with 120 channels, and Merged “DNA 8+ HTD 62”

## V. CONCLUSION

In this study we evaluated the impact of MPEG-7 textural features on the detection performance of an existing morphology-based CAD system for mammographic masses. Specifically, two types of the MPEG-7 textural descriptors were evaluated: 1- Edge histogram descriptor (EHD) 2- Homogeneous texture descriptor (HTD). ROC analysis showed that performance of the EHD-based neural network was low suggesting that the mammographic texture as captured by EHD is not particularly useful for the specific detection task. This finding is consistent with the fact that contrast modulation can be lost because of the large spatial frequencies present in a typical mammogram. It is possible that EHD could be more helpful if performed on enhanced ROIs.

Contrary, addition of the HTD features resulted in improved performance of the morphology-based CAD scheme suggesting the importance of texture for the detection task. Further investigation of more textural features using wavelet analysis is underway.

## REFERENCES

- [1] P. Ndjiki-Nya, O. Novychny, T. Wiegand, "Merging MPEG-7 descriptors for image content analysis", Proceedings of IEEE International Conference on Acoustics, Speech, and Signal Processing, vol. 3: iii – 453-456,2004.
- [2] B. S. Manjunath, Jens-Rainer Ohm, Vinod V. Vasudevan, and Akio Yamada, "Color and Texture Descriptors," IEEE Trans. On Circuits and Systemsfor Video Technology, vol. 11, No. 6, June 2001.
- [3] Su Jung Yoon, Dong Kwon Park, Soo-Jun Park, Chee Sun Won, "Image retrieval using a novel relevance feedback for edge histogram descriptor of MPEG-7," International Conference on Consumer Electronic, Los-Angeles, CA, pp. 354-355, 2001.
- [4] J. R. Ohm, F. Bunjamin, W. Liebsch, et al. "A multi-feature description scheme for image and video database retrieval," *IEEE 3<sup>rd</sup> Workshop on Multimedia Signal Processing*, Copenhagen Denmark, pp. 123~128, 1999.
- [5] Y. Deng, B. S. Manjunath, "Unsupervised segmentation of color-texture regions in images and video," *IEEE Trans. On Pattern Analysis and Machine intelligence*, vol: 23(8), pp. 800-810, 2001.
- [6] Chee Sun Won et al. "Efficient use of MPEG-7 edge histogram descriptor," *ETRI Journal*, vol. 23(8), pp. 23-30, 2002.
- [7] Yong Man Ro, Munchurl Kim, Ho Kyung Kang, B. S. Manjunath, and Jinwoong Kim, "MPEG-7 Homogeneous Texture Descriptor," *ETRI Journal*, vol. 23(2), pp. 41-51, 2001.
- [8] B. S. Manjunath, and W. Y. Ma, "Texture features for browsing and retrieval of image data," *IEEE Trans. Pattern Analysis and Machine Intelligence*, vol. 18, pp. 837-842, Aug. 1996.
- [9] Nevine H. Eltonsy, Georgia D. Tourassi, Piotr A. Habas, A. S. Elmaghraby, "DNA: Directional neighborhood analysis for detection of masses in screening mammograms," *SPIE Feb. 2005, San Diego, CA*, vol. 5747, p. 38, 2005.
- [10] Heath M., Bowyer K., Kopans D., et al., "Current Status of The Digital Database for Screening Mammography. In *Digital Mammography*, Kluwer Academic Publishers (1998).
- [11] Rumelhart, D.E., Hinton, G.E., Williams, R.J.: Learning internal representations by error propagation. in Parallel Distributed Processing: Explorations in the Microstructures of Cognition (Vol. 2). Edited by Rumelhart, D.E., and McClelland, G.L., (The MIT Press, Cambridge, MA, 1986), 318-362.
- [12] Hagan, M.T., Menhaj, M.: Training feed-forward networks with the Marquardt algorithm. *IEEE Trans Neural Networks* 5(6):989-993 (1994).
- [13] Efron, B., Tibshirani, R.J.: An Introduction to the Bootstrap, Monographs on Statistics and Applied Probability. ed. D. R. Cox et al. (Chapman & Hall, New York, NY, 1993).